Nuclei at high angular momentum

Nilsson, Sven Gösta

Published in:
Proceedings of the third General Conference of the European Physical Society, 1975

1975

ENERGY AND PHYSICS

Proceedings of the Third General Conference of the European Physical Society

9-12 September 1975
Bucharest, Romania

Published by European Physical Society
PO-Box 39, CH-1213, Petit-Lancy 2, Switzerland

Nuclei at High Angular Momentum *

S. G. NILSSON

Lund Institute of Technology, Lund, Sweden

Recent experimental progress in the use of heavy ions [1] (Stephens) has opened the interest for a theoretical study of very high-angular-momentum states in nuclei. Such a study, based solely on the liquid-drop model, was undertaken in 1972 by Cohen, Plasil and Swiatecki [2]. In this latter work many new features involving radical changes of shape at high angular momenta were exhibited. Recently some publications have also appeared where shell structure effects were added to the liquid-drop background through the works of the groups at Warsaw, Lund, Dubna and Jülich [3,4,5,6] (see also the preceeding work by Bohr and Mottelson [7]). In particular, the recent results of the Lund-Warsaw group will be reported here [4].

Parametrisation

The shape parametrisation is that defined by the equipotential surfaces of the modified harmonic oscillator of the type

$$V \sim \rho^2 \left[1 + \sqrt{\frac{5}{4\pi}} \frac{2}{3} \left\{ \varepsilon \cos\gamma \cdot Y_{20} + \frac{\varepsilon \sin\gamma}{\sqrt{2}} (Y_{22} + Y_{2-2}) \right\} + 2\varepsilon_4 Y_{40} \sqrt{\frac{9}{4\pi}} \right].$$

Thus the macroscopic calculations correspond to shapes defined in terms of ε, γ and ε_4 in such a way that to each point ε and γ and given angular momentum I, the total classical energy, i.e. surface + Coulomb + rotational energy, is minimized with respect to ε_4. The rotational energy is evaluated in terms of classical rigid rotation around the x-axis. The potential-energy surfaces appropriate for ^{154}Sm are shown in Fig. 1 and the equilibrium shape trajectories in the ε, γ plane are exhibited in Figs. 2 and 3 for ^{154}Sm and ^{158}Yb respectively. As was found by the authors of ref [1], the transition from oblate to triaxial shapes takes place between I = 78 and 80 and between I = 70 and 72 for ^{154}Sm and ^{158}Yb, respectively.

* based on work by R. Bengtsson, S. E. Larsson, G. Leander, P. Möller, I. Ragnarsson, S. Åberg, S. Szymanski, S. G. Nilsson and G. Andersson, to be published [4].

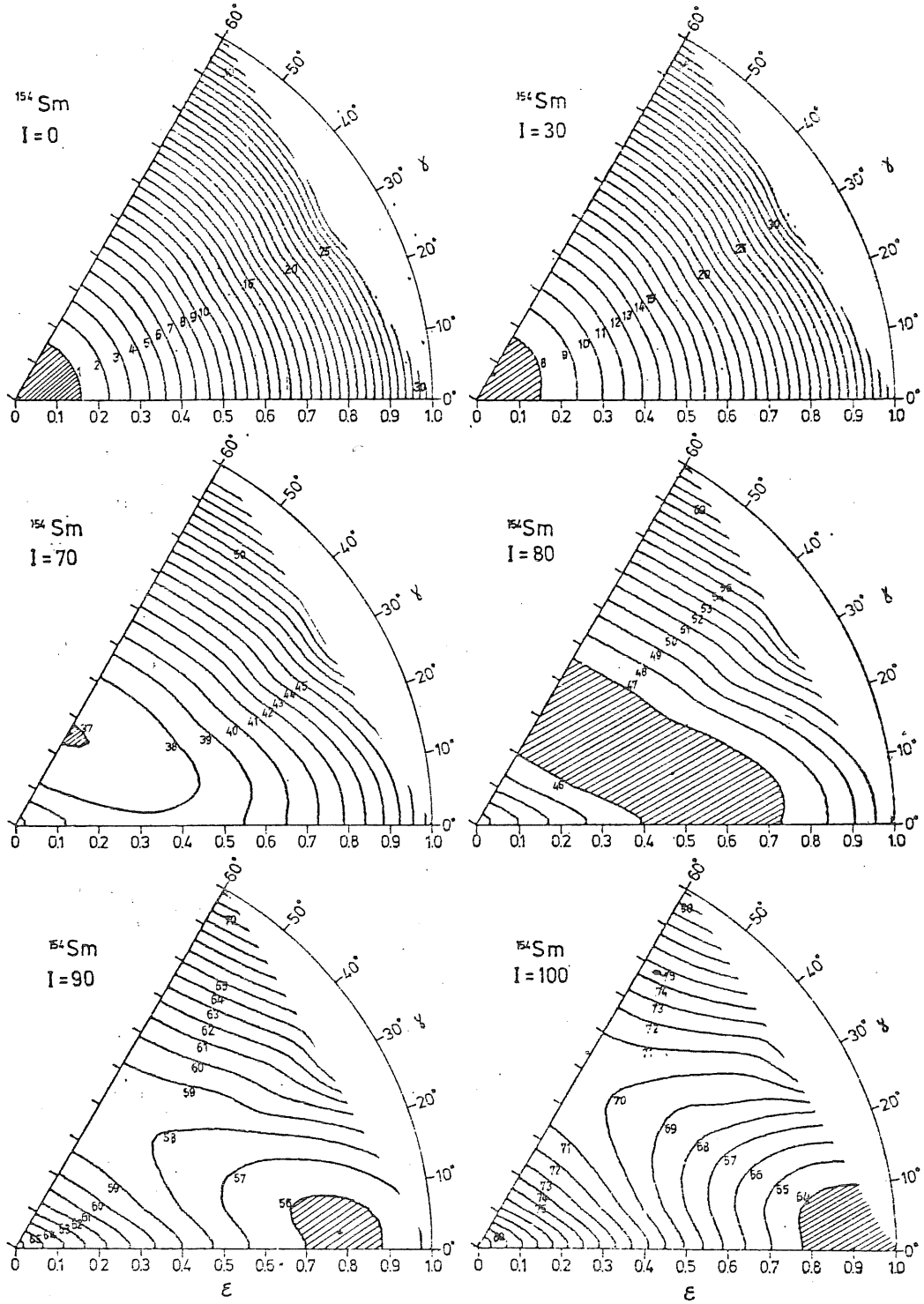

Fig. 1. The classical energy surface in ε, γ for ^{154}Sm for a sequence of I-values. A minimisation with respect to ε_4 is made for each ε and γ. The rotational energy is that of a rigid rotor around the x-axis.

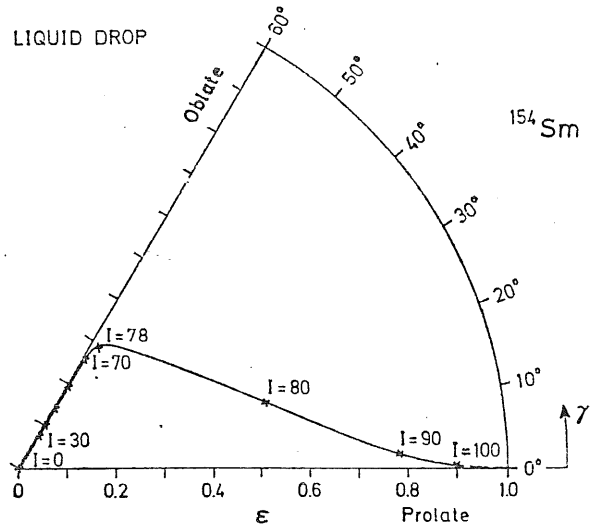

Fig. 2. The equilibrium trajectory of the classical equilibrium shape for ^{154}Sm (x = 0.526).

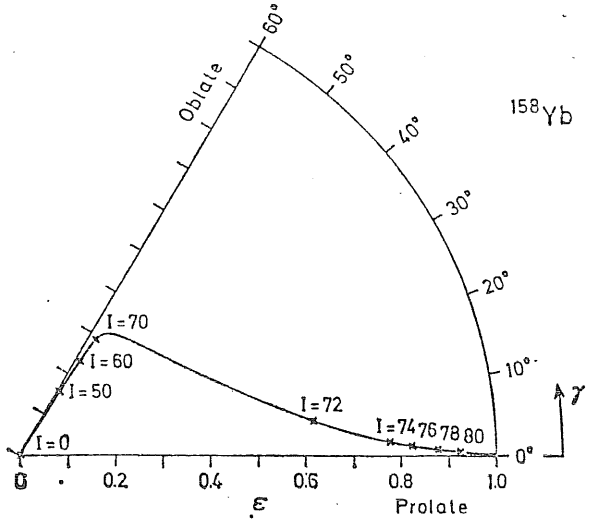

Fig. 3. The same as Fig. 2 but for ^{158}Yb.

It is interesting to plot the minimum (shape-optimised) classical energy as a function of I (the different shapes are then reflected in different parts of the curve). We have as an alternative chosen to exhibit the usual plot of the second derivative $\frac{\partial E}{\partial I^2}$ or $\frac{K^2}{2J}$ vs. the first derivative $\frac{\partial E}{\partial I}$, the latter being $K\omega$. The "shape tran-

sition" point near I = 80 is then dramatically projected as a "super back-bend" (Fig. 4).

These results are now strongly modified with the inclusion of so-called shell effects. The latter are calculated on the basis of the modified-oscillator model with

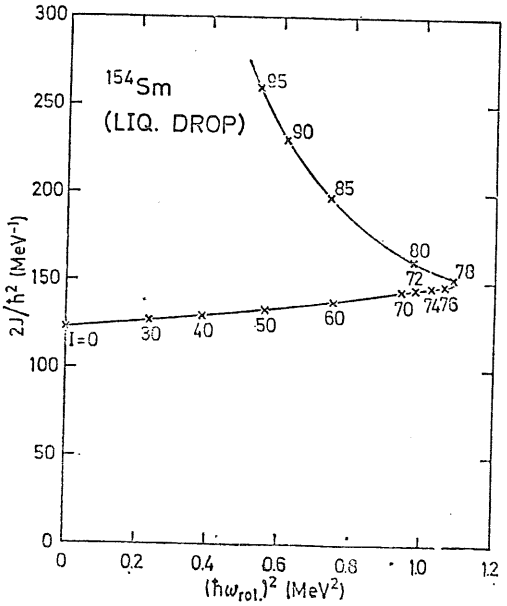

Fig. 4. Super-back-bending. The classical relation between $\left(\frac{\partial E}{\partial I^2}\right)^{-1}$ and $(K\omega)^2$ for ^{154}Sm.

the inclusion of $\vec{l}^2$ and $\vec{l}\cdot\vec{s}$-terms. Furthermore, the auxiliary condition of a given angular momentum is taken into account by the addition in the generator Hamiltonian H_ω of a term ωI_x, where ω is a Lagrangian multiplier. The quantity ω also has the physical meaning of the rotational frequency. The term ωI_x can then be thought of as the Hamiltonian form of the Coriolis and centrifugal contributions in the rotating system.

We have thus

$$H_\omega = H - \omega I_x = \Sigma\, h_\omega$$

to which corresponds the eigenfunction ψ^ω in the form of a Slater determinant of eigenfunctions of h_ω. The energy and angular momenta corresponding to ψ^ω are determined as

$$<\psi^\omega|H|\psi^\omega> = E(\omega)$$

and

$$<\psi^\omega|I_x|\psi^\omega> = I(\omega)$$

respectively.

These expressions are now compared to those obtained for Strutinsky smeared energies and angular momenta. Purely reflecting the positions of the energy levels Jennings [8] defines an energy distribution function

$$g_1(e^\omega) = \sum_i \delta(e^\omega - e_i^\omega)$$

while angular momentum distribution by Jennings is reflected in a function

$$g_2(e^{\omega}) = \sum_i <m>_i \delta(e^{\omega} - e_i^{\omega}).$$

These are easily generalised to the smeared case as

$$\tilde{g}_1(e'^{\omega}) = \int S(e'^{\omega} - e^{\omega})\, g_1(e^{\omega})\, de^{\omega}$$

and

$$\tilde{g}_2(e'^{\omega}) = \int S(e'^{\omega} - e^{\omega})\, g_2(e^{\omega})\, de^{\omega}.$$

From these one can calculate

$$\tilde{I} = \int \tilde{g}_2\, de^{\omega}$$

and

$$\tilde{E} = \int \tilde{g}_1\, de^{\omega} + \omega \tilde{I}.$$

On the basis of these expressions, for each value of ω one obtains a set of $I(\omega)$ and $E(\omega)$, from which a curve $E = E(I)$ can be defined. Intermediate values are subsequently obtained by interpolation. Similarly, from $\tilde{I}(\omega)$ and $\tilde{E}(\omega)$ a "smooth" curve, $\tilde{E} = \tilde{E}(\tilde{I})$, can be constructed. To define the latter only two or three points

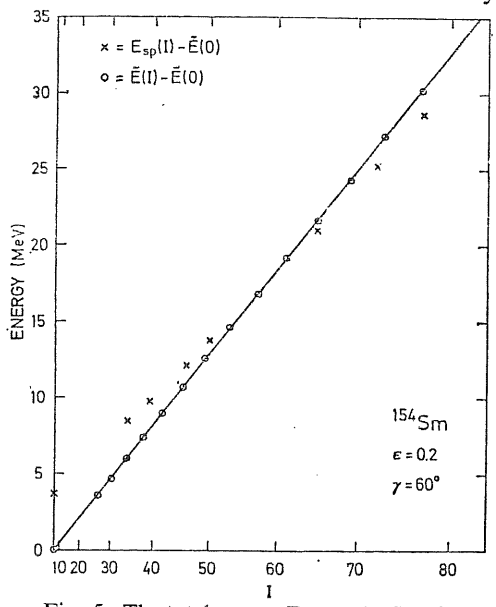

Fig. 5. The total energy E and the Strutinsky smeared total energy $\tilde{E}$ as functions of angular momentum for given ε and γ.

are required due to the fact that for the Strutinsky case, as already stated, a very straight line in $\tilde{E}$ vs. $\tilde{I}^2$ is obtained. The difference for constant I between E and $\tilde{E}$ is defined as the shell energy for each I-value, see Fig. 5. It is to be noted that E_{shell}

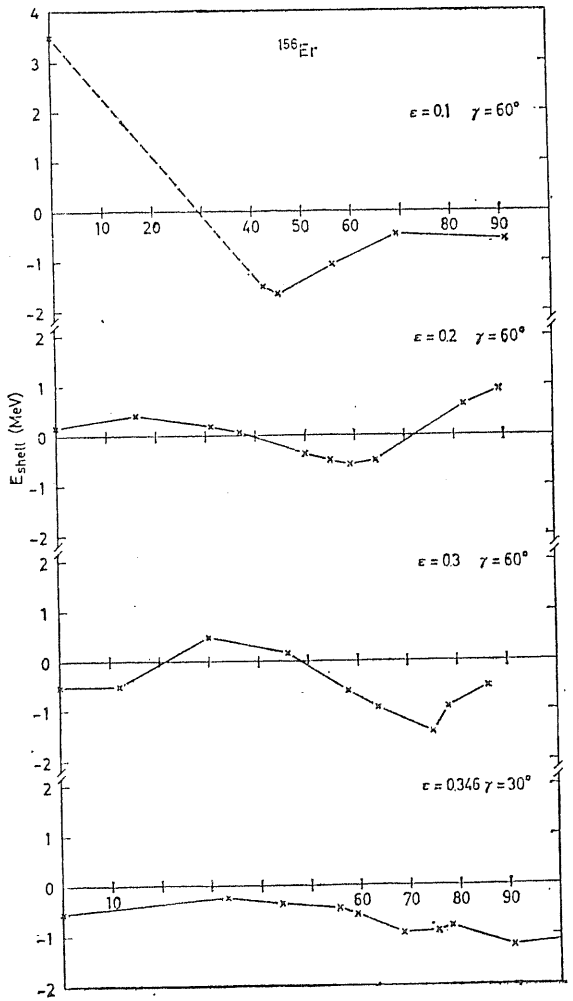

Fig. 6. E_{shell} as a function of I for given ε and γ.

Fig. 7. The "dynamical inertia" $\frac{\partial E}{\partial I^2}$ and the "rigid inertia" as the slope in E vs I^2 diagrams for the H.O. and M.O. cases.

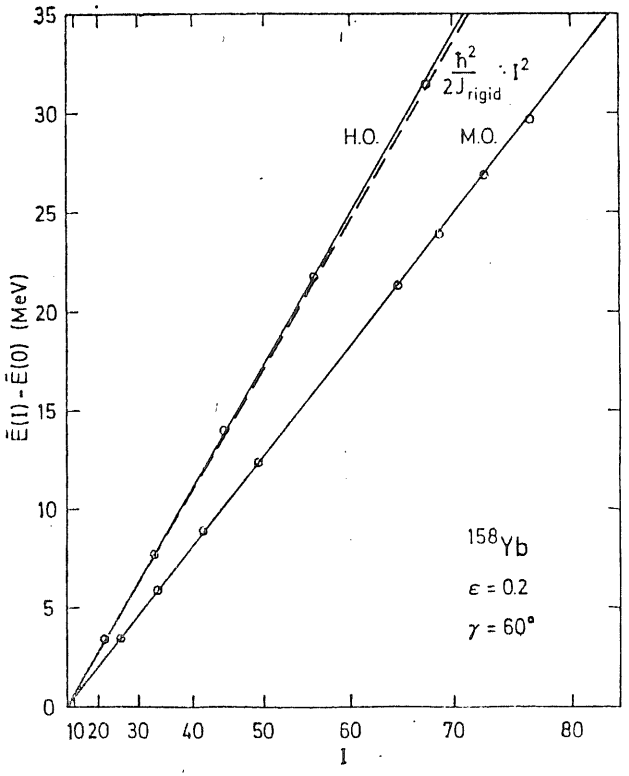

for $I \neq 0$ also includes shell contributions to the rotational moment of inertia. In fact a separation between "intrinsic shell energy" and "rotational shell energy" cannot be made. From Fig. 6 one can also note that E_{shell} changes drastically with I for given ε and γ. In fact a negative shell energy usually goes positive with a change of I of 50—100 units. The period of E_{shell} in I is of the order of $\Delta I \simeq 100-200$.

From the relation between E and I for given deformation, one may define a "dynamical" inertia, as plotted in Fig. 7 for a few s.p. potentials, namely, the pure harmonic oscillator and the modified oscillator with $(\vec{l}^2 - <\vec{l}^2>)$. Finally, also the relation between E and I corresponding to the expectation value of the "rigid" inertia $\rho(z^2 + y^2)d\tau$ is given as the dashed line, where the integration is done over an equipotential surface for constant density.

The excess of the M.O. dynamic moment of inertia over the rigid value, as first pointed out in ref [3], is found to be a spurious and undesirable effect due to the $\vec{l}^2$ term, as first illucidated by Mottelson [9], Brack [10], Leander [11], Hamamoto [12] and the authors of ref [4]. In our calculations the Strutinsky method is employed for the rotating case and thereby the "smeared" inertia value is replaced by the rigid equivalent.

Calculational results

We turn now to the final results. Calculations have been performed for about thirty rare-earth nuclei with $Z = 62-70$ and thirty nuclei in the region $Z = 72-82$, i.e. below ^{208}Pb. The energy surfaces are based on a grid in ε and γ of 40 points. Ten different ω-values up to $\omega/\omega_0 = 0.14$ are used. Based on these ω-values the values of E_{shell} are thus obtained by interpolation for values of I equal to 30 to 90 (usually) in steps of 10. For the sake of simplicity, it is assumed over the entire region that pairing can be neglected. Independent calculations by the Jülich group [6] bear out that pairing collapses for $I \geqslant 30$. Beyond this point the present approximation should thus apply satisfactorily.

For this set of I-values one can now obtain the total energy as

$$E(I, \varepsilon, \gamma) = E_{liq}(\varepsilon, \gamma, \varepsilon_4^{min}) + E_{shell}(\varepsilon, \gamma) + E_{rot}(\varepsilon, \gamma, \varepsilon_4^{min}).$$

The total energy is subsequently plotted as a function of ε and γ (with the liquid-drop energy minimized with respect to ε_4; in the most recent calculation ε_4 is also included for the shell energies). In this way surfaces corresponding to Figs 8—9 are obtained for ^{160}Yb and ^{192}Pt. In some of these cases also the region of negative γ-values, $\gamma = 0-20°$, is of some interest, as first pointed out by the authors of ref [5]. Such extended surfaces have also been constructed by the Lund group. They are to be presented in ref [4].

Finally, also trajectories for the equilibrium shape of a sequence of nuclei corresponding to the yrast energies have been constructed and are exhibited in Figs 10—11.

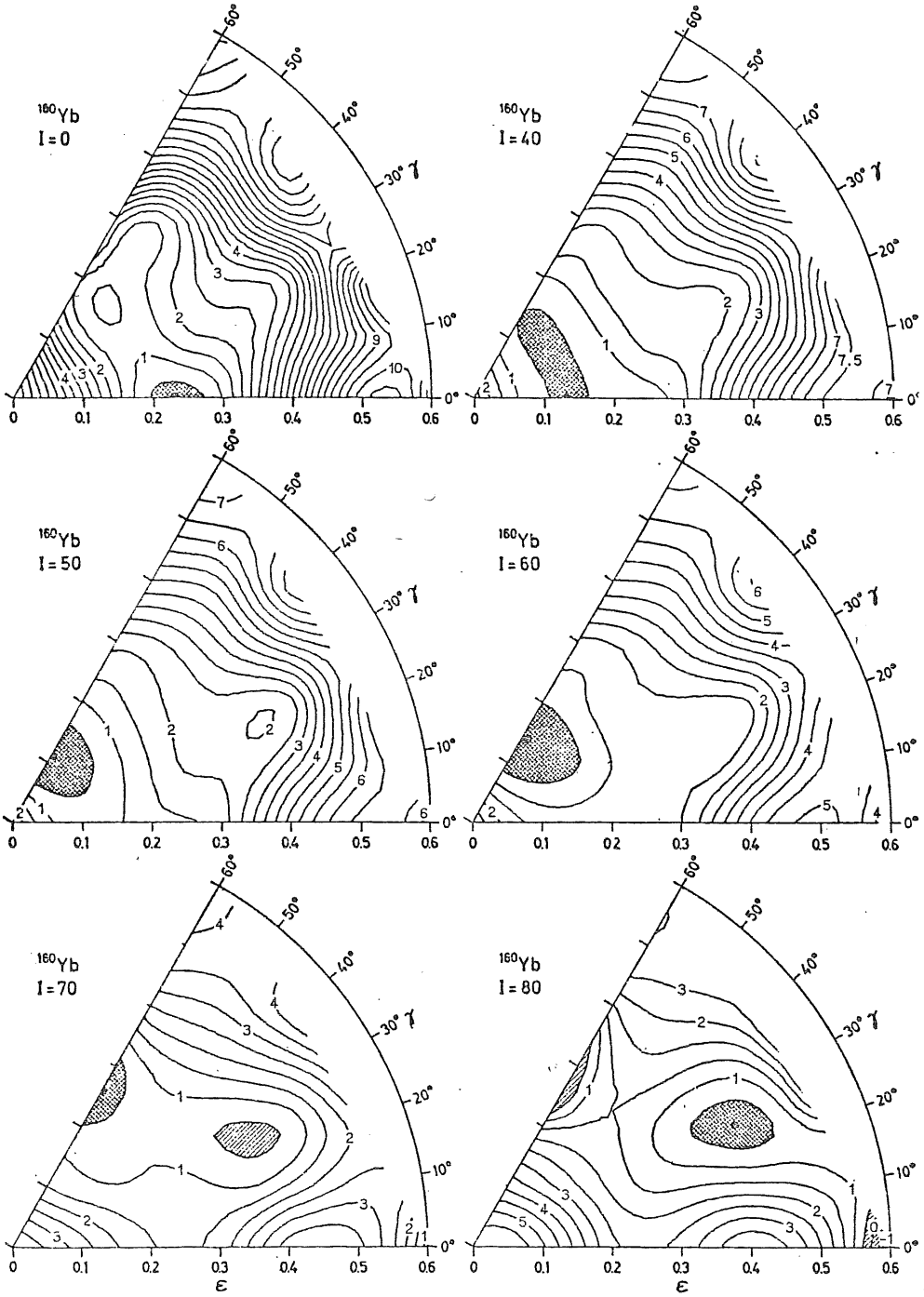

Fig. 8. The total-energy surface (with no pairing included) as a function of I, ε and γ (with the ε_4 degree of freedom included for the liquid-drop and rigid rotational-energy terms) for the nucleus ^{160}Yb.

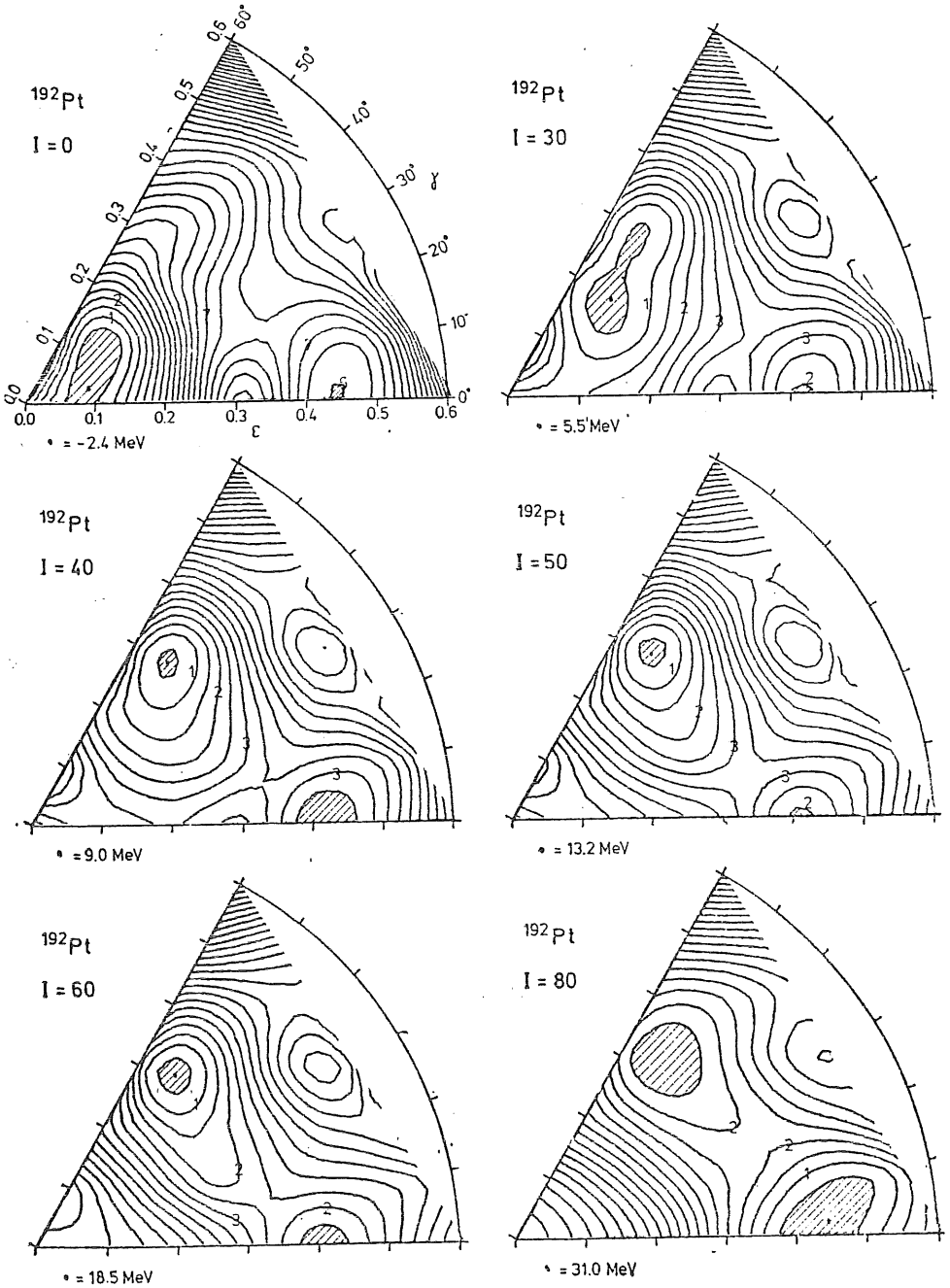

Fig. 9. The same as Fig 8 but for ^{192}Pt.

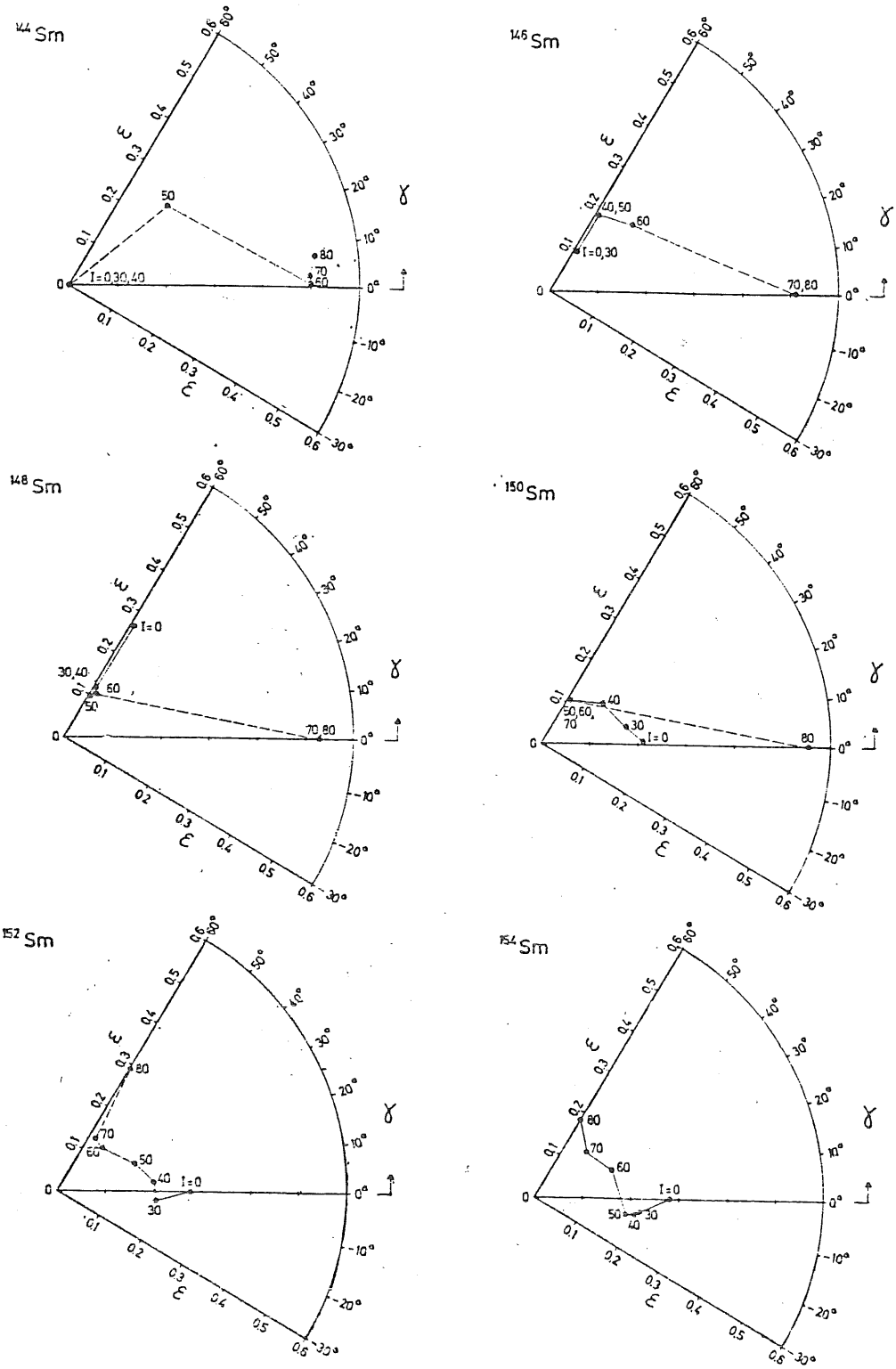

Fig. 10. Equilibrium shape trajectories for isotopes of Sm.

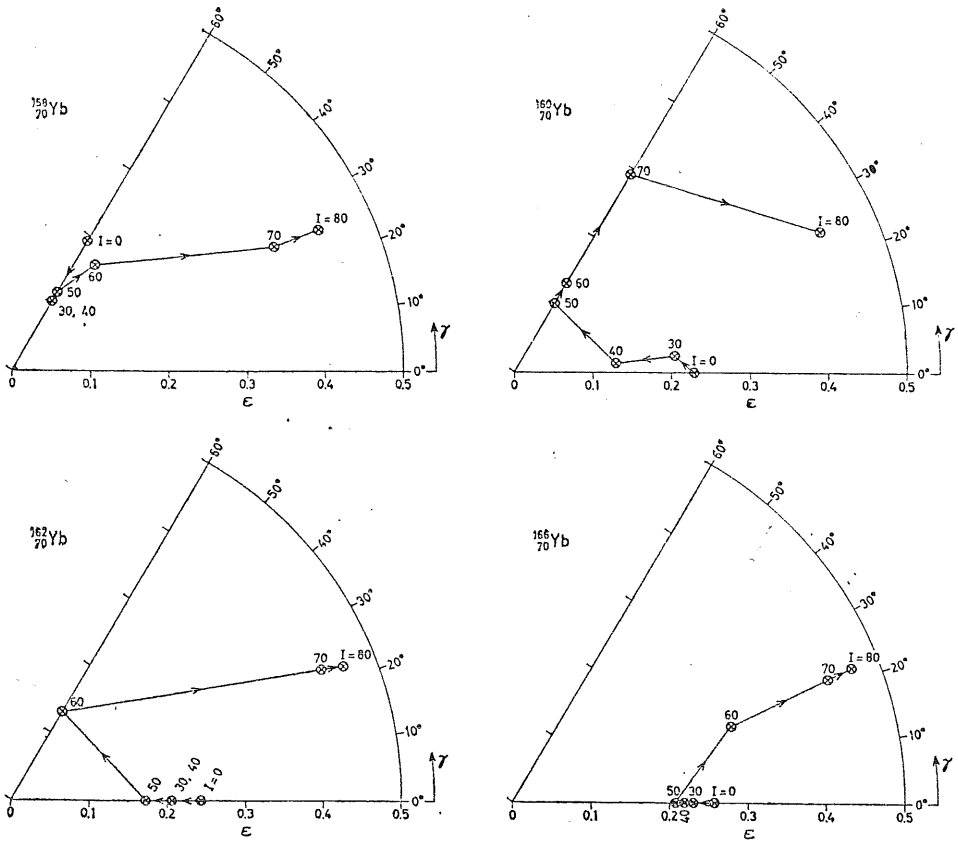

Fig. 11. The same as Fig 10 but for isotopes of Yb (negative γ not included).

Summary of results

One may summarize the most interesting results as follows for the $150 < A < 208$ region of nuclei as calculated by us.

a) Consider first the nuclei with neutron number less than 100 and A less than 170. For the nuclei near the beta stability line, the trajectory stays largely near the prolate axis before the shape finally turns triaxial with increasing I. These nuclei also tend to initially contract in ε for, say, I increasing from 0 to 40. Furthermore the trajectory involves negative γ-values over certain intermediate I-values.

b) In the same mass region $A < 170$ the very neutron-deficient nuclei in certain regions of I have a trajectory along the $\gamma = 60°$ axis. Here "yrast traps" appear to have a certain likelihood to occur.

c) For the mass region $170 < A < 208$ the negative γ-values play a minor role. Furthermore the trajectories of those nuclides that are clearly prolate in their ground state and have $N > 100$ tend to "stretch" in deformation, i.e. move along

the $\gamma = 0$ axis with ε *increasing* with I (contrary to the light rare earths). Other nuclides that already in the ground state are prolate but nearly γ-unstable tend to shift their equilibrium over to $\gamma = 50-60°$ with increasing I before finally turning prolate. (^{192}Pt is an example.)

A detailed analysis of the microscopic mechanisms behind the encountered behaviour can be found in the forthcoming paper [4] by the Lund group. The co-operation of Profs. Aage Bohr and Ben Mottelson as well as Drs. V. Pashkevich and K. Nergaard is highly appreciated.

References

1 M. V. BANASHIK, R. S. SIMON, P. COLOMBANI, D. P. SOROKA, F. S. STEPHENS and R. M. DIAMOND, *Phys. Rev. Lett. 34* (1975) 892.
2 S. COHEN, F. PLASIL and W. J. SWIATECKI, *Ann. of Phys.* (New York) *82* (1974) 557.
3 R. BENGTSSON, S. E. LARSSON, G. LEANDER, P. MÖLLER, S. G. NILSSON, S. ÅBERG and Z. SZYMANSKI, *Phys. Lett. 57B* (1975) 301.
4 R. BENGTSSON, S. E. LARSSON, G. LEANDER, P. MÖLLER, I. RAGNARSSON, S. ÅBERG, Z. SZYMANSKI and S. G. NILSSON, to be published.
5 K. NERGAARD and V. V. PASHKEVICH, Jülich Conference – 16 (vol. I, 1975) p. 59 and private communication, May 1975.
6 A. FAESSLER, K. R. SANDHYA, F. GRÜMMER and K. W. SCHMID, Jülich conference –16 (vol. I, 1975) p. 60.
7 A. BOHR and B. R. MOTTELSON, *Physica Scripta 10A* (1974) 13.
8 R. K. JENNINGS, to be published.
9 B. MOTTELSON, private communication.
10 M. BRACK and P. QUENTIN, to be published.
11 G. LEANDER, private communication.
12 I. HAMAMOTO, private communication.